INTERNATIONAL JOURNAL FOR NUMERICAL METHODS IN FLUIDS
Int. J. Numer. Meth. Fluids 2003; **43**:93–114 (DOI: 10.1002/fld.609)

Assessment of conservative weighting scheme in simulating chemical vapour deposition with trace species

J.-S. Wu*,†,‡, W.-J. Hsiao§, Y.-Y. Lian§ and K.-C. Tseng§

Department of Mechanical Engineering, National Chiao-Tung University, Hsinchu 30050, Taiwan

SUMMARY

Low-pressure or ultra-high vacuum chemical vapour deposition often involves important trace species in both gas-phase and surface reactions. The conservative weighting scheme (J. Thermophys. Heat Transfer 1996; **10**(4):579) has been used to deal with the trace species often involved in some non-reactive physical processes, which is otherwise considered computationally impossible using the conventional DSMC method. This conservative weighting scheme (CWS) improves greatly the statistical uncertainties by decreasing the weighting factors of trace-species particles and ensures the conservation of both momentum and energy between two colliding particles with large difference of weighting factors. This CWS is further extended to treat reactive processes for gas-phase and surface reactions with trace species, which is called extended conservative weighting scheme (ECWS). A single-cell equilibrium simulation is performed for verifying both the CWS and ECWS in treating trace species. The results of using CWS show that it is most efficient and accurate for weight ratio (trace to non-trace) equal to or less than 0.01 for flows with two and three species. The results of a single-cell simulation using ECWS for gas-phase reaction and surface reactions show that only ECWS can produce acceptable results with reasonable computational time. Copyright © 2003 John Wiley & Sons, Ltd.

KEY WORDS: LPCVD; conservative weighting scheme; extended conservative weighting scheme; trace species; reactive; single-cell simulation

1. INTRODUCTION

1.1. Fundamentals of CVD process

Chemical vapour deposition (CVD) is one of the principal unit operations in microelectronics processing [1]. It has been applied in many ways such as the formation of thin film of metals, semiconductors and insulating materials of high purity, encompassing a wide range of material properties. The basic principle of CVD is that a suitable combination of reactant gases is

*Correspondence to: J.-S. Wu, Department of Mechanical Engineering, National Chiao-Tung University, 1001 Ta-Hsueh Road, 30050 Hsinchu, Taiwan.
†E-mail: chongsin@cc.nctu.edu.tw
‡Associate professor.
§Graduate research assistant.

Received 17 April 2002
Revised 22 January 2003

brought in contact with a wafer surface that is maintained at an elevated temperature. Gas-phase precursor(s) may or may not react or decompose homogeneously into different gas-phase species depending upon the operating conditions. One or more of the gas-phase species reacts heterogeneously at the surface to deposit a solid film. Usually the activation energy of the decomposition process is provided by the thermal energy of the wafer. It is generally agreed that a number of required steps, which must take place in the deposition sequence affecting the film growth [2], including: (a) Transport of precursor(s) to the deposition zone; (b) Surface adsorption of the precursor(s); (c) Transformation of the precursor(s) to film constituent; (d) Incorporation of film constituent into crystal lattice (film growth); (e) De-sorption of reaction by-products; (f) Transport of by-products away from the deposition zone.

1.2. Modelling of CVD process

The studies about modelling CVD process can be divided into two major categories. One is the study of the macro-scale analysis. This is about the whole flow filed in the reactor, i.e. the spatial distribution of velocity, energy and density from the viewpoint of reactor size. These were evaluated by the Navier–Stokes equations [3–7] or the DSMC method [8–11]. The use of Navier–Stokes equations is most effective when the flow conditions are well in the hydrodynamic regime. In contrast, the DSMC method [18] is efficient in the slip and transitional regimes, and is the only viable method in transitional regime. In addition, it is much easier to incorporate micro-scale physical models in the DSMC method. If the flow conditions are in the transitional regime, DSMC is the most popular method employed in this category, e.g. References [12, 13]. However, in the actual CVD process these physical phenomena strongly interact each other and the multi-scale analysis must be needed. For example, the angular distribution of the precursor molecular velocity and energy at the wafer surface is critical in determining the step coverage quality in trench or via holes. This information can be provided through the reactor-scale simulation. In addition, gas-phase chemistry influences the precursor compositions at the wafer surface, which in turn changes the uniformity of deposited film at the wafer surface. Therefore, a numerical approach suited to treat multi-scale process in CVD is required. Indeed, the direct simulation Monte Carlo (DSMC) method is one of the best choices among the candidates.

DSMC is a physically accurate particle method for the computation of non-equilibrium gas flows. The technique is most useful in circumstances where there are insufficient numbers of collisions in the flow to maintain the equilibrium forms of the distribution functions describing the various energy modes of the gas. Generally, such conditions prevail when the average distance between successive collisions of each particle, the mean free path, is comparable to the characteristic length scale of the flow. This type of non-equilibrium condition occurs in a variety of problems of current interest. These include hypersonic flows around vehicles flying at high altitude in planetary atmospheres, e.g. Reference [14], flows from small rockets used on satellites for control, e.g. Reference [15], flows involved in the synthesis of thin films, e.g. Reference [16], and flows in micro-scale mechanical structures, e.g. Reference [17], to name a few.

Since the particle-based nature of the DSMC method, it is well suited to handle the flows and reactions in CVD process. Applying the DSMC method to simulate CVD process is generally divided into two parts, i.e. gas-phase (homogeneous) and surface (heterogeneous) reactions. In the gas-phase reaction, collisions are handled on a probabilistic basis. Within

each cell, potential collision partners are randomly selected without regard to their relative positions. A collision is performed if their collision probability exceeds some random fraction. And so does the chemical reaction if the steric factor exceeds another random fraction [18]. This process is repeated until the correct collision rate is obtained in each cell. Only binary collisions are considered as the diluteness of the gas makes any three-body collisions highly improbable. Additionally, in the surface reaction, the reaction can be simulated depending on the reactive probability, γ, using the same concept as in the gas-phase. This reactive probability may depend on the species concentration near the wafer surface [3, 5] or impinging energy of the precursor [19].

It is unfortunate that the chemical species of most importance in CVD process often occur in very small quantities. The amount of the trace gas, for example, SiH_2, existing in CVD is usually very small for low-pressure environment, on the order of 10^{-4} or even smaller for the mole fraction. Similar situation occurs in plasma-enhanced CVD flows. This presents a major difficulty to the DSMC algorithm. To simulate one particle of the trace gas in a computational cell at this mole fraction would require simulation of 10 000 other particles. This approach would therefore require at least 10 million particles or even more for a simulation of modest size. Even with a numerically efficient DSMC code implemented on parallel computers, this simulation would require hundreds of hours or even more of execution time. To circumvent this difficulty, a conservative weighting scheme (CWS) was developed by Boyd [20] for the DSMC technique in which the physical weight of a particle W depends upon its chemical species. Thus, a particle representing a trace species would be given a lower weight than particles representing more abundant species. The scheme can also be extended to treat the chemical reaction for the steric factor in gas-phase and the reactive probability of the surface reaction, which we call extended conservative weighting scheme (ECWS) [21].

In summary, the objectives of the current research are listed as follows: (1) to implement and to assess a conservative weighting scheme for the DSMC method treating the trace species non-reactive gas flow; (2) to implement and to assess an extended conservative weighting scheme to deal with both gas-phase and surface reactions in a model CVD process.

2. NUMERICAL METHOD

2.1. The DSMC method

The basic idea of DSMC is to calculate practical gas flows through the use of no more than the collision mechanics. The molecules move in the simulated physical domain so that the physical time is a parameter in the simulation and all flows are computed as unsteady flows. An important feature of DSMC is that the molecular movement and intermolecular collisions are uncoupled over the time intervals that are much smaller than the mean collision time. Both the collision between molecules and the interaction between molecules and solid boundaries are computed on a probabilistic basis and, hence, this method makes extensive use of random numbers. In most practical applications, the number of simulated molecules is extremely small compared with the number of real molecules. In general, the procedure of DSMC method consists of four major steps: moving, indexing, collision and sampling. In the current study, the variable hard sphere (VHS) model [18] and no time counter (NTC) [18] are used to

simulate the molecular collision kinetics. The details of the procedures and the consequences of the computational approximations are well documented in Bird's monograph [18] and thus are not repeated here.

2.2. Conservative weighting scheme (CWS) for non-reactive flows

Under equilibrium conditions, a species-dependent weighting scheme proposed by Bird [22] will approximately conserve linear momentum and energy over a sufficiently large number of collisions. However, the scheme does not conserve these properties explicitly at each collision as clearly demonstrated by Boyd [20]. Indeed, Bird [22] recommended against the use of this scheme. Hence, there is a requirement for developing a weighting scheme for the DSMC technique that does conserve explicitly linear momentum and energy.

To overcome the problem mentioned above, Boyd [20] proposed a conservative weighting scheme, which is described briefly in the following. The first stage of the conservative weighting scheme is to split the particle of abundant species (W_1) into a particle with weight W_2 (trace species) and a particle with weight of W_1–W_2 when two particles (trace and abundant species) collide. Then, a collision is performed using the conventional DSMC procedure for the two particles that have the same weight W_2. The final stage is to merge together the two particles that were split such that the each linear momentum in three physical directions is exactly conserved. Unfortunately, it does not explicitly conserve total energy. But the energy difference (loss) caused by this split-merge process is found to be proportional to the weight ratio W_2/W_1 (<1). Thus, the conservative weighting scheme proposed by Boyd [20] nearly conserves total energy as this weight ratio is much smaller than unity. The split-merge process described in the above can be summarized as Figure 1.

It was argued that if the split-merge scheme is employed at each collision, then energy is continuously lost from the system because of energy loss [20]. Boyd [20] also proposed some practical remedies to keep this energy loss to a minimum by adding lost energy to the central-mass energy in a subsequent collision. In general, this energy should only be added to collisions between particles having the maximum weight used in the simulation to keep this effect a minimum; that is, between two non-trace particles (leading to a non-trace collision). Thus, energy conservation is essentially maintained for each iterative step of the simulation.

2.3. ECWS for chemical reactive flows with trace species

In the following, we will briefly describe the homogeneous gas-phase and heterogeneous surface chemical reaction involved in the CVD process (e.g. the silicon vapour deposition) and the details of corresponding ECWS we will use to handle these processes.

2.3.1. ECWS for homogeneous gas-phase reaction. Consider a model gas-phase reaction as follows:

$$AB + M \leftrightarrow A + B + M \tag{1}$$

where AB is the trace species (e.g. SiH_4), M is any abundant species (e.g. H_2), A is the most trace species (e.g. SiH_2) and B is the decomposed gas (e.g. H_2) in the current study.

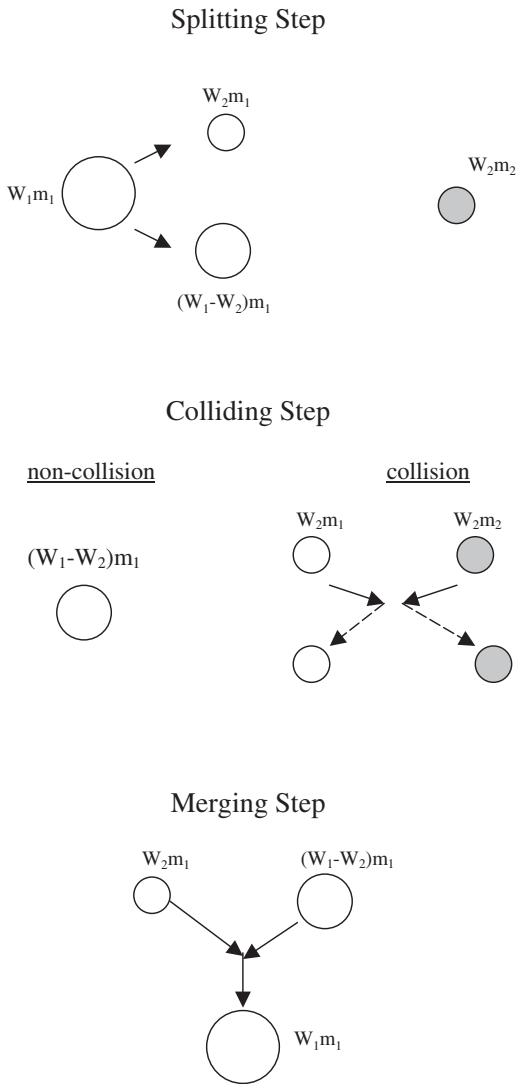

Figure 1. Schematic diagram of CWS for non-reactive flow.

In the following, we will describe how to implement ECWS considering chemical reactions in DSMC simulation. The basic idea for treating homogeneous decomposition is to decrease gradually the weights of reactants for every reactive collision [2]. Figure 2 shows the schematic diagram of ECWS for treating trace species in reactive flows. In summary, ECWS consists of three main steps as described in the following.

Splitting step: The first step is to divide *AB* particle and *M* particle into two parts, respectively, as shown in Figure 2. The one with superscript 'r' is the part of reactive collision, while the other with superscript 'n' represents the part of non-reactive collision. If we

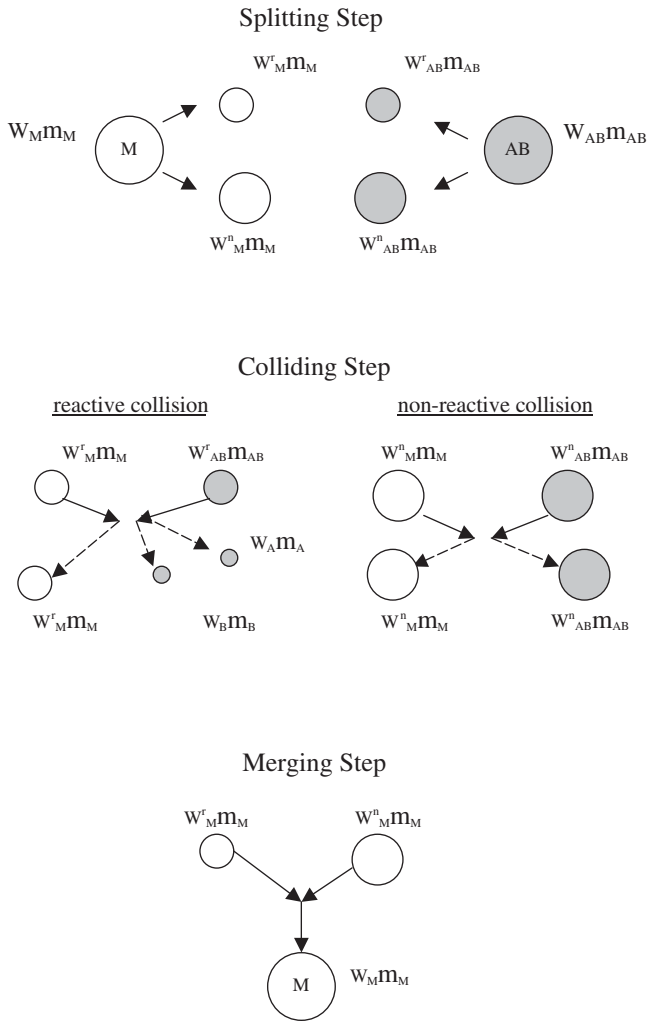

Figure 2. Schematic diagram of Extended CWS for treating homogeneous decomposition with trace species.

assume that a particle AB is a collection of N_{AB} $(= W_{AB}/W_A)$ *equivalent* particles (one *equivalent* particle is equal to one particle A), then the number of *equivalent* particles involved in each chemical reaction is

$$N^r_{AB} = W_{AB}/W_A P_r = N_{AB} P_r \tag{2}$$

where P_r is the reaction probability, where the format depends upon the model used (e.g. TCE model [18] as used in the current study unless otherwise specified). This means that N^r_{AB} *equivalent* particles out of N_{AB} particles are involved in each reaction. Furthermore, the weighting factor for reactive and non-reactive part of AB (or M) particle can be expressed

respectively as

$$W_{AB}^r = W_M^r = N_{AB}^r \tag{3}$$

$$W_{AB}^n = W_{AB} - N_{AB}^r, \quad W_M^n = W_M - N_{AB}^r \tag{4}$$

Note that mass conservation is strictly satisfied during the splitting process. In addition, W_{AB}^r $(= W_M^r)$, W_{AB}^n and W_M^n vary depending upon the flow conditions during each collision.

Colliding step: Collisions are then performed using the conventional DSMC method for both parts as illustrated in the middle part of Figure 2. First, we consider the reactive part of the collision. The reaction model [e.g. TCE model in the current study] can be applied with AB^r and M^r having the same weight, and species A and B are created with the weight factor W_A and W_B, respectively. The number of the created A and B particles is W_{AB}^r. Though *equivalent* particles AB^r vanishes, the other *equivalent* particle M^r still remains with the weight factor of W_M^r. Non-reactive part of the collision between particles with weight factors of W_M^n and W_{AB}^n is handled using CWS, which is the same as that described in previous section. Therefore, all the post-collision states (velocities and energies) of all particles can be determined. In the current method, mass conservation is, however, enforced by decreasing the weight factor of AB particle, rather than by consuming the number of AB particles.

Merging step: The last step is to determine the velocity and energy of third body M as shown in Figure 2. Two *equivalent* particles, M^r and M^n, have the velocity vectors, C_M^r and C_M^n, having the different weights, W_M^r and W_M^n, respectively. Again, by applying CWS, we can merge the two *equivalent* particles. The final velocity vector C_M' is evaluated as

$$C_M' = (1 - \phi)C_M^n + \phi C_M^r \tag{5}$$

where $\phi = N_{AB}^r / W_M$. The energy loss between the pre- and post-collision states can be readily derived as

$$\Delta E = \sum_i m_M \phi(1 - \phi) C_i^n C_i^r \tag{6}$$

This energy loss is added by the same way as CWS. It is noted that this energy loss is small if ϕ is much less than unity, which is always the case in the reaction of silane decomposition. The inelastic collision involving internal energy can be determined similarly.

It is noted that each particle of products A and B will be created each time step with the appropriate weight factors and the conservation of momentum (exactly) and energy (nearly) is satisfied at each collision by ECWS.

The conventional formulation of the steric factor (TCE model) for the VHS gas model first proposed by Bird [23] depends on the internal contributed degree of freedom as

$$P_r\left(\frac{E_c}{kT}\right) = \frac{\pi^{1/2}\alpha\Lambda T_{\text{ref}}^{\eta}}{2\sigma_{\text{ref}}(kT_{\text{ref}})^{\eta-1/2+w}} \frac{\Gamma(\varepsilon + 2 - w)}{\Gamma(\varepsilon + \eta + 3/2)} \left(\frac{m_r}{2kT_{\text{ref}}}\right)^{1/2} \frac{(E_c - E_a)^{\eta+\varepsilon+1/2}}{E_c^{\varepsilon+1-w}} \tag{7}$$

where α has a value of one for like and two for unlike collision partners, Λ and η are constants, σ_{ref} defines a reference cross section at a temperature T_{ref}, k is Boltzmann's constant, $w = \omega_{ab} - 1/2$, where ω_{ab} is the viscosity–temperature exponent that is specified for collisions between molecules of species A with those of species B, ε is the average number of internal degrees of freedom, and E_a is the activation energy of the reaction. For procedures of gas-phase particle collisions considering chemical reactions, see Figure 3 for details.

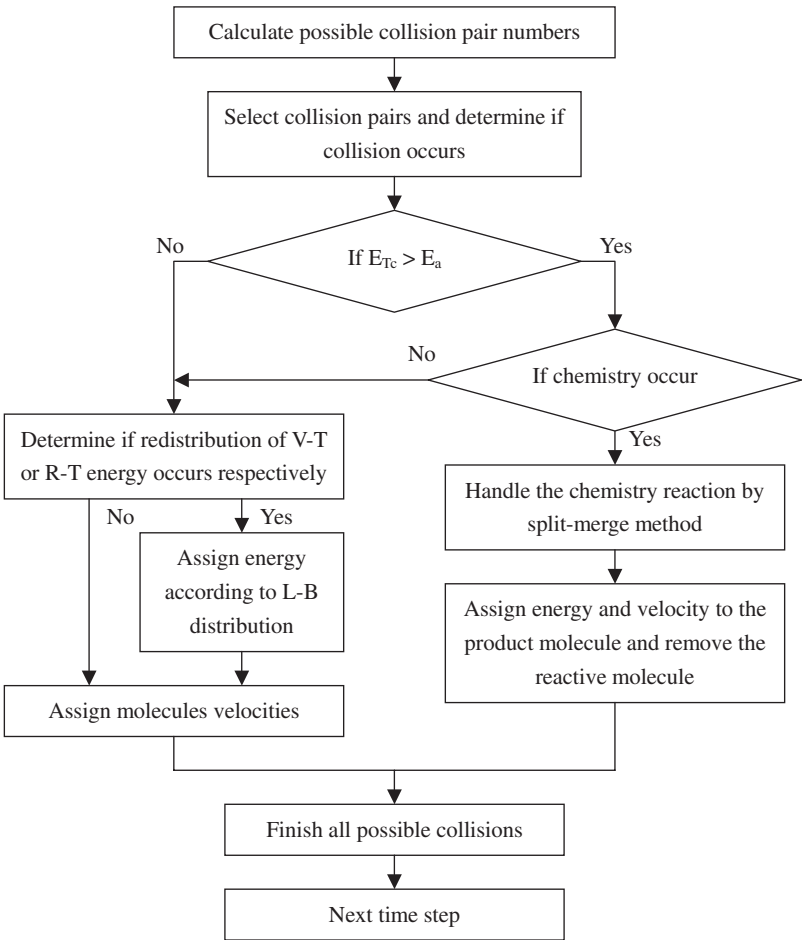

Figure 3. Sketch of flow chart for gas-phase particle collision.

2.3.2. ECWS for heterogeneous surface reaction. Consider two model surface reactions:

$$AB \rightarrow C + 2B \tag{8}$$

$$A \rightarrow C + B \tag{9}$$

where, for example, A stands for SiH_2, B for H_2, AB for SiH_4 and C for Si in silane-based silicon vapour deposition. To simplify the calculation, we consider the model of Moffat [6], a non-linear Arrhenius temperature dependence, for the surface reaction probability of AB (e.g. silane). In addition, we set the surface reaction probability for the highly reactive open shelled molecule A (e.g. SiH_2) to one as presented in Reference [6].

In the DSMC simulation, if γ is much smaller than unity, enormous computational time is required to achieve reasonable sample size on the surface. Similar to the gas-phase reaction, we use extended CWS to circumvent these problems. Consider the case that a computational

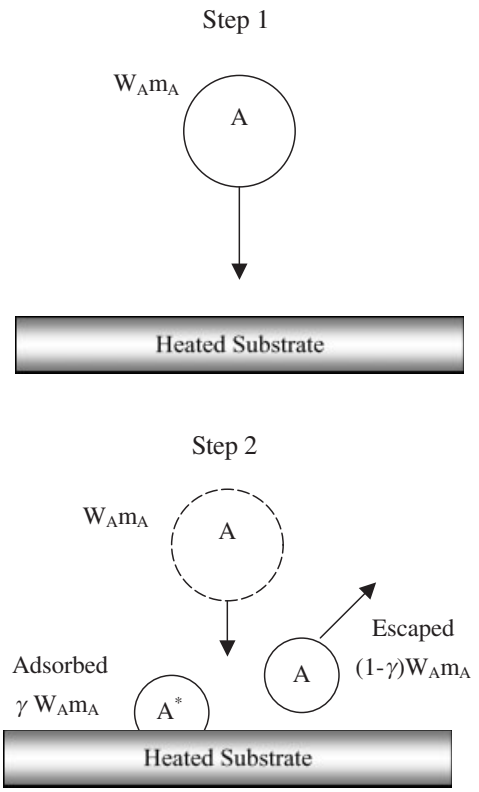

Figure 4. Schematic diagram of Extended CWS for treating heterogeneous reaction.

species A with weight W_A being adsorbed to the surface with the probability γ. If we assume that a computational particle A is a set of W_A *equivalent* particles, the number of *equivalent* particles that are adsorbed to surface every time the particle A hits the surface is expected as

$$W_A^S = W_A \gamma \tag{10}$$

where the superscript S represents the surface related properties. Then the computational particle A is divided into two parts again, as shown in Figure 4. That is, one part is adsorbed to the surface with weight W_A^S, and another escapes from the surface with weight $W_A - W_A^S$ which enforces the conservation of mass.

3. RESULTS AND DISCUSSIONS

In the following, we have performed the single-cell DSMC simulation for non-reactive and reactive flows by using CWS, variable weighting scheme by Bird [22] and constant weighting scheme, respectively. By comparing the velocity distribution, chemical reaction rate coefficient and deposition distribution, it can be clearly shown that CWS is much superior to the conventional scheme if trace species is involved.

3.1. Simulation for two-component mixture without chemical reactions

The first simulation includes two species: Ar and He with different weight ratios. In this simulation, we would like to know the effectiveness and accuracy of the conservative weighting scheme for non-reactive flows. We perform the simulation with different weight ratios using variable weighting scheme by Bird [22], constant weighting scheme and CWS, respectively. The total simulation particles are 10 000 in the cell, and the weight ratios are $W_{Ar}/W_{He} = 0.1$ (10%), 0.05 (5%) and 0.01 (1%), respectively. Note that the number in the parenthesis represents mole fraction of Ar. Thus, Ar is a potential trace species in this case. The temperature in the cell is preset as 1000 K. Figures 5 and 6, with weight ratios of 1/9 and 1/19, respectively, show the velocity distribution after 20 000 time steps. It is clear that the conventional scheme (constant weighting) performs better than both the variable weighting scheme by Bird [22] and CWS. This is because CWS has energy loss from non-trace gas, and we must add the lost energy to non-trace gas. When the weight ratio is not small enough, the energy loss will be relatively large, and hence it will affect the energy distribution. In turn, the velocity distribution will deviate strongly from the expected M–B (Maxwell–Boltzmann) distribution, which it should be in the current test case. But when the weight ratio is equal to or less than 0.01, as shown in Figure 7, the CWS can perform as accurately as the conventional scheme (constant weighting) once the weight ratio is equal to or less than 0.01, while the variable weighting scheme by Bird [22] shows some over-sampling at the velocity of zero. Figures 8–10 illustrate the relative error as a function of simulation time for the two-species case with $W_{Ar}/W_{He} = 0.1$, 0.05 and 0.01, respectively. Note that the relative error is defined as the root mean square of the sum of deviation from the M–B distribution relative to the M–B

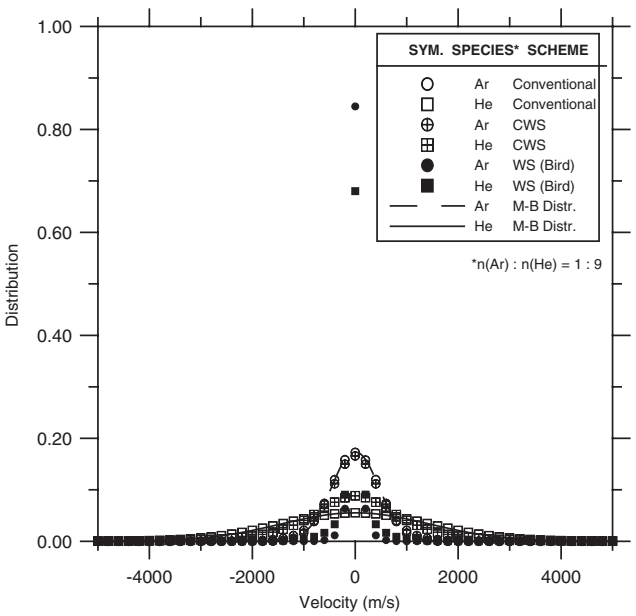

Figure 5. Velocity distribution with weight ratio 1:9.

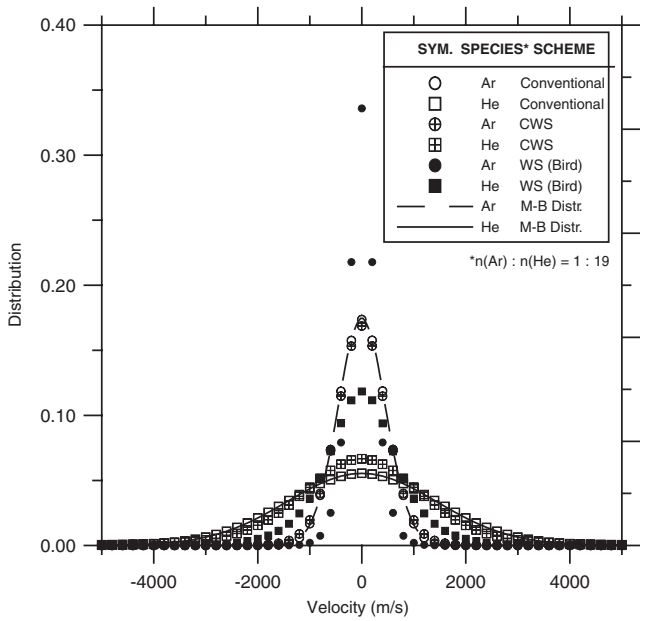

Figure 6. Velocity distribution with weight ratio 1:19.

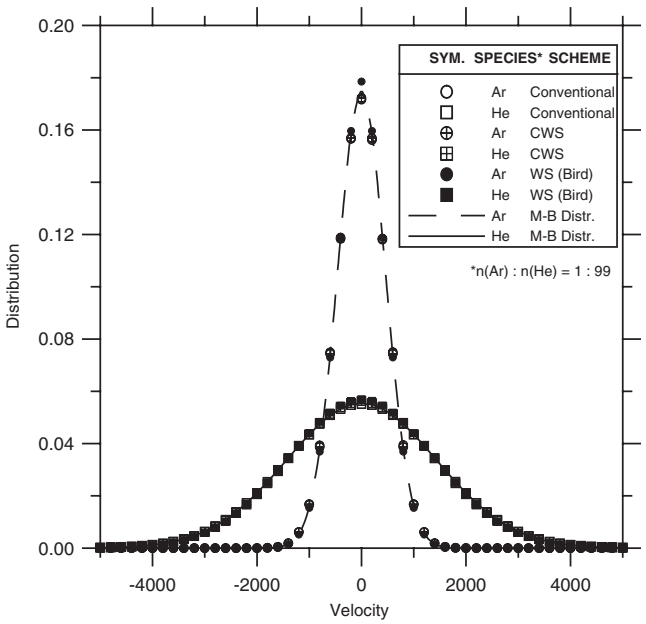

Figure 7. Velocity distribution with weight ratio 1:99.

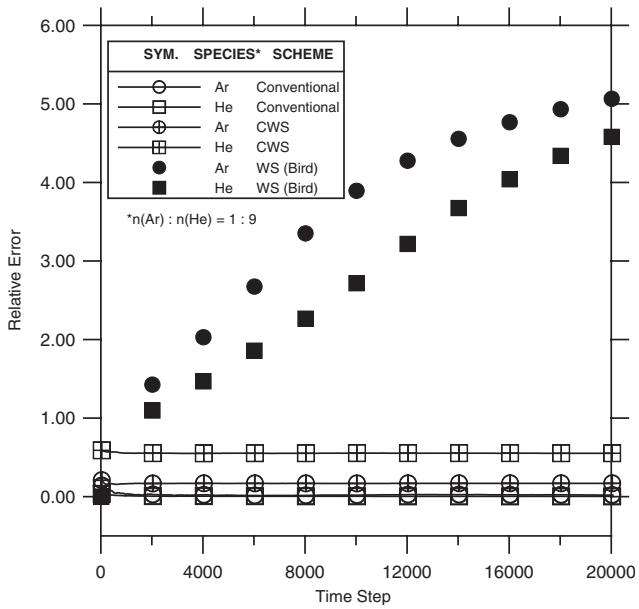

Figure 8. Relative error as a function of the number of simulation time steps with weight ratio 1:9.

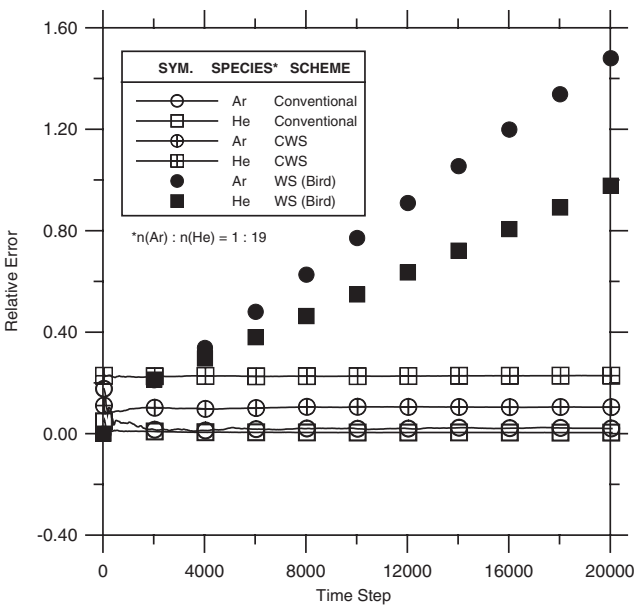

Figure 9. Relative error as a function of the number of the simulation time steps with weight ratio 1:19.

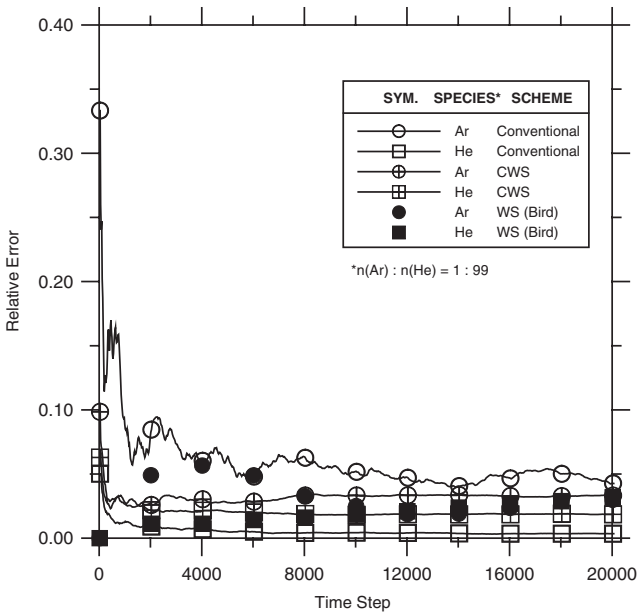

Figure 10. Relative error as a function of the number of the simulation time steps with weight ratio 1:99.

distributions by dividing the velocity range (-5000–$5000\,\mathrm{m/s}$) into 50 sections. In the case of weight ratio 0.01, the relative errors of both species by the CWS decrease to a reasonably low value in a few time steps, while that of trace species by the conventional method maintains unacceptably large as simulation continues. In the long run, the variable weighting scheme [22] achieves about the same level of errors as the CWS, however, it progresses with much higher errors in the early stage of simulation, which should be caused by the non-conservation of momentum and energy in each collision mentioned previously. This result shows not only the CWS is as accurate as the constant weighting scheme but is also very effective for dealing the flow involving trace species with the weight ratio equal to or lower than 0.01.

3.2. Simulation for three-component mixture without chemical reactions

This simulation includes three species, Ne, Ar and He, with weight ratio 1:99:9900 in order. The simulation conditions are similar to those of the two-species case. The total simulation particles increase up 100 000, and the temperature in the cell is kept at 1000K. Figure 11 shows the velocity distribution after 20 000 time steps for all three schemes. It clearly demonstrates that the conventional scheme (constant weighting) is incapable of handling the trace species in the period of simulation time because very few collisions of Ne–Ne occur in the cell. Again the velocity distribution by the variable weighting scheme [22] approximately fits the M–B curve, but with an over-sampling at the velocity of zero, which is similar to that in two-species simulation. Figure 12 shows the relative errors of both the trace species (Ar) and the most trace species (Ne) by the conventional scheme (constant weighting) are too large and decrease very slowly. As for the variable weighting scheme [22], similar situation as that

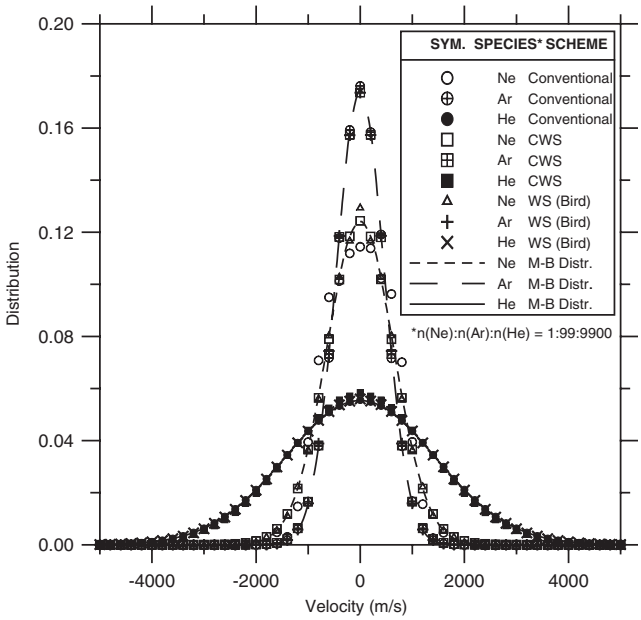

Figure 11. Velocity distribution with weight ratio 1:99:9900.

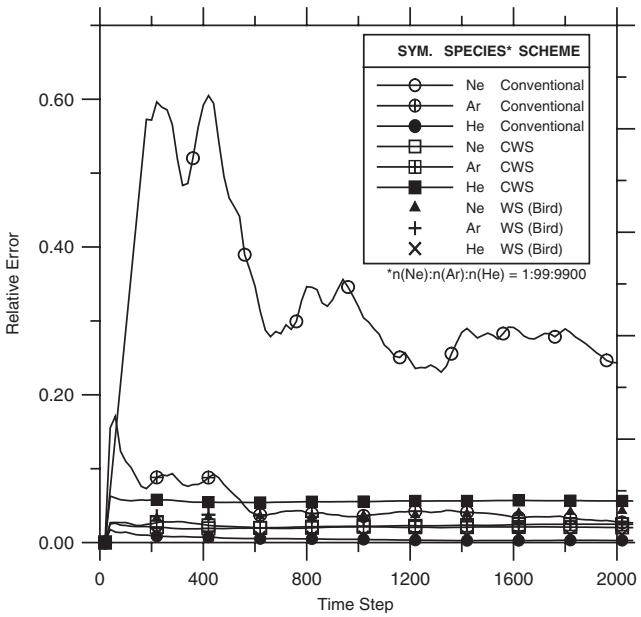

Figure 12. Relative error as a function of the number of the simulation time steps with weight ratio 1:99:9900.

of two-species simulation occurs. Thus, it is clear that the CWS performs much better than the conventional schemes if trace species are involved in DSMC simulation.

3.3. Simulation with gas-phase reaction

In this simulation, we would like to know if ECWS could reproduce the correct chemical reaction rate for before its application to the modelling of practical reactive flows. The gas is a mixture of SiH_4 (1%, trace species) and H_2 (99%) initially in a single cell. The initial total simulation particles are 20 000. The temperature in the cell varies from 800 to 1500 K, which will change the reaction rate accordingly. We use total collision energy model (TCE) proposed by Bird [18]. Note that the variable weighting scheme [22] is not performed in the following simulations for reactive flows. It lies in the fact that the large number of simulated molecules at the same position and with the same velocities (once reaction (1) occurs in the variable weighting scheme) will definitely cause serious bias problems in the collisional phase in a statistical simulation like DSMC, in addition to the non-conservation of momentum and energy during collision.

Figure 13 shows the chemical reaction rate coefficient K_f calculated by TCE model using theoretical Arrhenius law (related coefficients from Kleijn [3]), conventional scheme (constant weighting) and CWS as a function of temperature. Note that total internal degree of freedom (IDOF) is selected as 11. Both the conventional scheme and ECWS agree well with the theoretical value in the range of 1000–1500 K. It is, however, clear that the number of time steps to accumulate reasonable sample size for the conventional scheme is much larger than that of CWS (about two order of magnitudes larger), as shown in Figure 14. It becomes nearly impossible to use the conventional scheme for practical computations especially at lower temperatures, (800 and 900 K). In the current case, data of the conventional scheme are not shown (Figures 13 and 14) due to the inhibitive long computational time.

Figure 15 shows the variations of the predicted rate coefficient as a function of simulation time steps at 1200 K (IDOF = 11). It is clear that the rate coefficient computed by the conventional scheme does not coincide with theoretical value even after a long period of time,

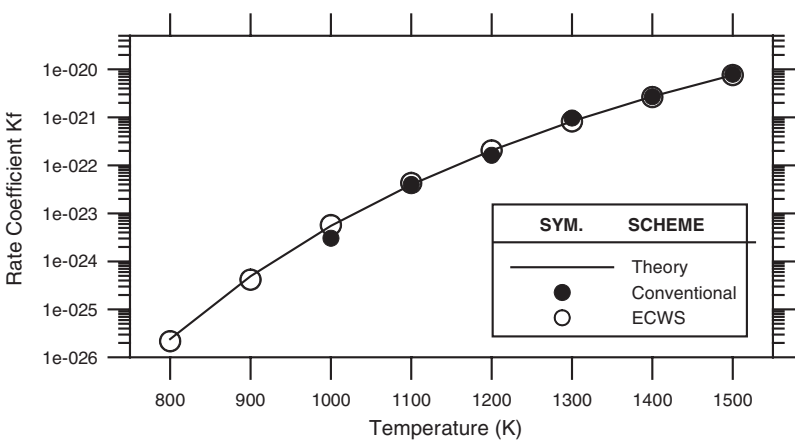

Figure 13. Rate coefficient K_f calculated by TCE model (IDOF = 11).

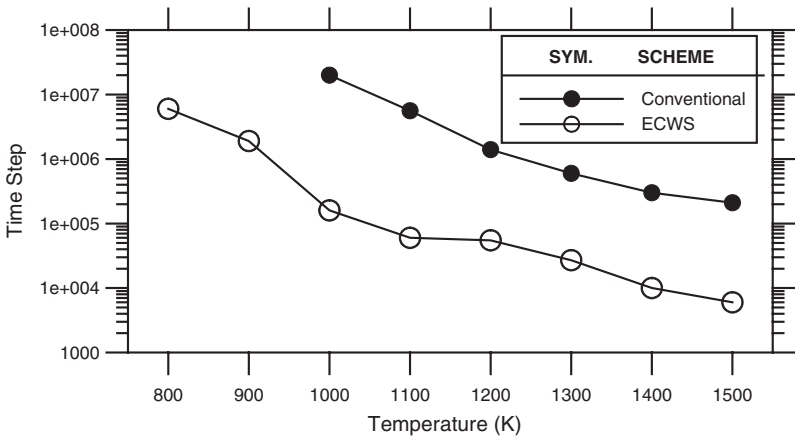

Figure 14. Number of time steps required to approximate theoretical value of rate coefficient (IDOF = 11).

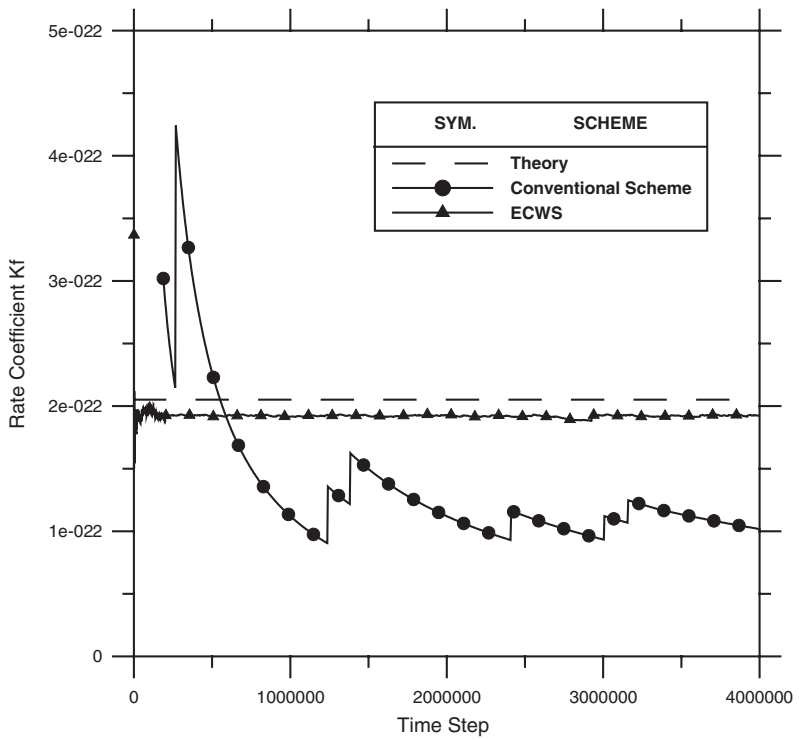

Figure 15. Rate coefficient K_f as a function of simulation time steps calculated (conventional scheme and ECWS at 1200 K, IDOF = 11).

Table I. Rate coefficient K_f computed by CS and ECWS, and simulation time steps and associated errors as compared with theoretical value.

Temp. (K)	K_f (Theory)	K_f (CS*)	Error (%) (CS)	Time steps (CS)	K_f (ECWS†)	Error (%) (ECWS)	Time steps (ECWS)
800	2.40E − 26	—	—	—	2.17E − 26	−9.58	6 000 000
900	4.91E − 25	—	—	—	4.15E − 25	−15.48	1 900 000
1000	5.49E − 24	3.03E − 24	−44.81	20 000 000	5.68E − 24	3.46	160 000
1100	3.96E − 23	4.01E − 23	1.26	5 600 000	4.29E − 23	8.33	60 000
1200	2.05E − 22	1.62E − 22	−20.98	1 400 000	2.04E − 22	−0.49	55 000
1300	8.26E − 22	9.69E − 22	17.31	600 000	8.21E − 22	−0.61	27 000
1400	2.73E − 21	2.69E − 21	−1.47	300 000	2.64E − 21	−3.30	10 000
1500	7.61E − 21	7.90E − 21	3.81	210 000	7.60E − 21	−0.13	6000

*CS = conventional scheme.
†ECWS = extended conservative weighting scheme.

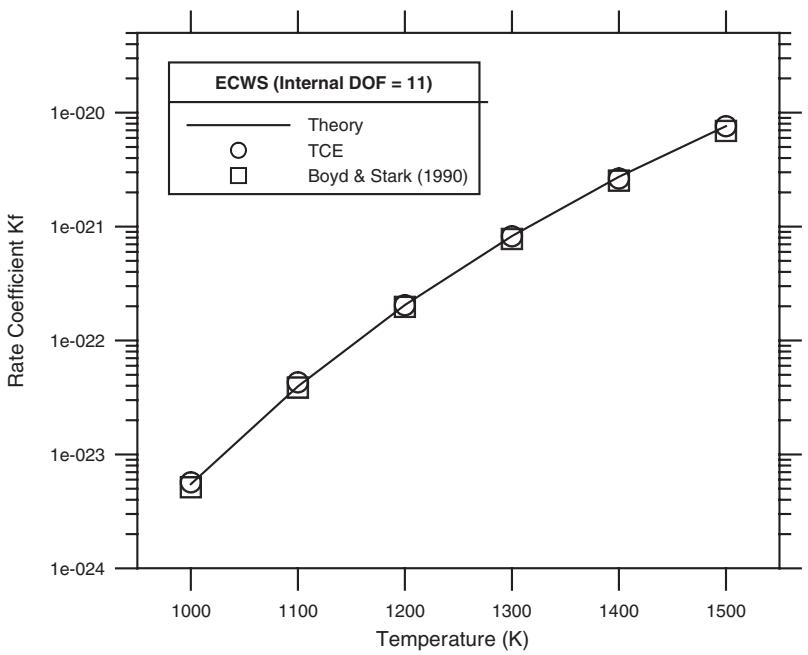

Figure 16. Rate coefficient calculated by ECWS, internal DOF = 11.

e.g. 4 million time steps due to the very low collision probability in the current test case. The rate coefficient, predicted by ECWS, however, reaches the theoretical value very fast and stays at the approximately constant value afterwards as simulation continues. Table I presents the errors and time steps required for sampling by the conventional scheme and ECWS. It can be seen clearly that ECWS is superior to the conventional scheme for simulating chemical reaction involving trace species.

To identify the effects of IDOF using ECWS, Figures 16 and 17 present the rate coefficients (by ECWS) as a function of the temperature for total internal degree of freedom of 11 and 3,

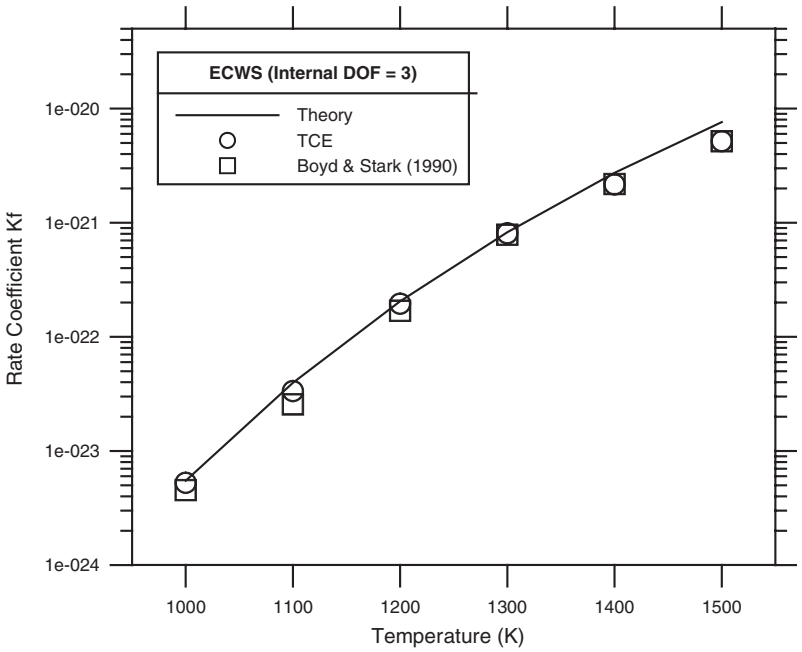

Figure 17. Rate coefficient calculated by ECWS, internal DOF = 3.

respectively. The results show that the prediction of rate coefficient by TCE along with the model proposed by Boyd and Stark [19] for IDOF = 11 are both in good agreement with the theoretical value in the temperature range of 1000–1500 K. However, it deviates from the theoretical value if IDOF = 3 is used, especially in the higher temperature range (1400–1500 K). This may be caused by the increasing importance of internal degree of freedom at higher temperature. This has also been observed and confirmed by Hsu [24], where he has shown that DSMC simulation, using internal DOF = 11, can reproduce the theoretical rate coefficient in the similar temperature range.

3.4. Simulation with surface reaction

The number of initial simulation particles in a single cell is 100 000, and the temperature is 1500 K in the gas as well as at wall. Only the bottom wall is able to have surface reactions. It is divided into 25 sections for counting the deposited particles. Figure 18 shows the total number of deposited particles on the surface at different surface reaction probability after 20 time steps of simulation. It is clear that ECWS produces about 100 times as many deposited particles compared with the conventional scheme within 20 time steps of simulation for all the γ considered. This improvement reduces greatly the statistical uncertainties of evaluating deposition uniformities on the surface otherwise caused by the low surface reaction probability.

Figure 19 presents the number of simulation time steps required as a function of the surface reaction probability within a preset uniformity tolerance. This tolerance is defined as the sum

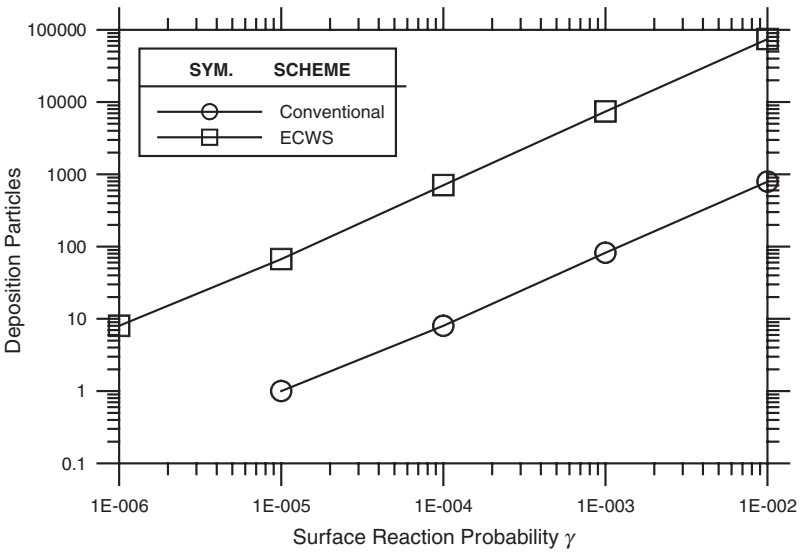

Figure 18. Number of deposited particles on the surface as a function of surface reaction probability γ, after 20 time steps.

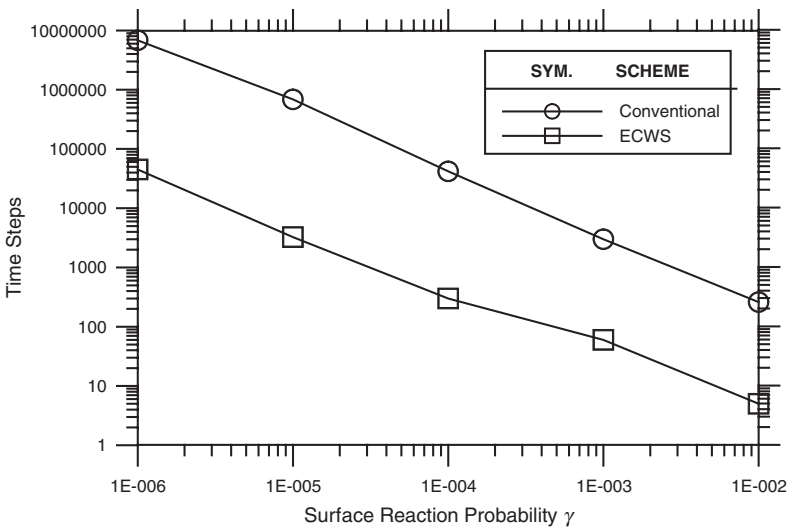

Figure 19. Number of time steps to obtain acceptable surface reaction probability γ (normalized error < 0.8).

of the normalized absolute differences (between average and local value) for all deposited sites on the surface. In the simulation, the preset tolerance is set as 0.8. It is clear that the conventional scheme generally requires two order-of-magnitude large number of time step to achieve preset uniformity on the surface.

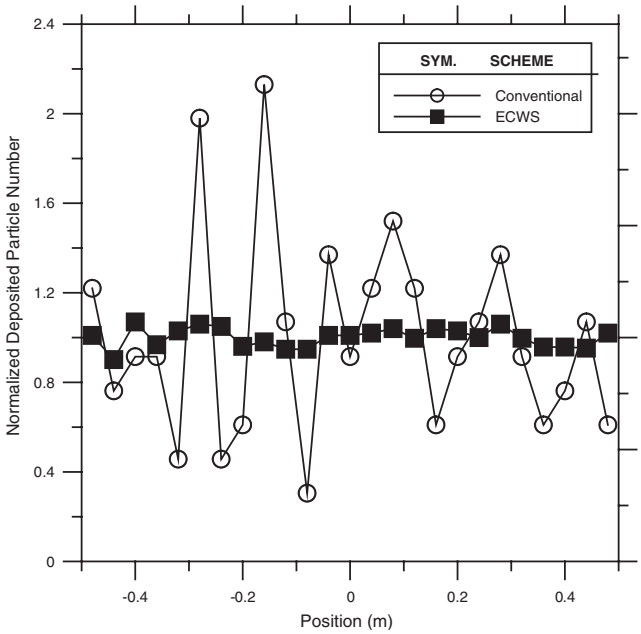

Figure 20. Spatial distribution of normalized deposited particle number for $\gamma = 10^{-3}$.

Figure 20 illustrates the spatial distribution of normalized deposited particle number along the surface. It is again clear that the uniform distribution of deposited particle number can be more or less reproduced using ECWS. On the contrary, the results become unacceptable using the conventional scheme for case of low surface reaction probability.

In summary, the above verifications have clearly demonstrated the superiority of CWS over the conventional scheme in simulating chemical reaction process (both homogeneous and heterogeneous) involving trace species.

4. CONCLUSIONS

In the current study, the conservative weighting schemes (CWS and ECWS) are assessed to handle the trace species in the DSMC simulation with and without chemical reaction using a single-cell simulation. In summary, the major findings of the current research are listed as follows:

1. CWS is shown to be effective and accurate in DSMC simulation without chemical reaction for two-species and three-species mixtures with concentration ratio (trace to abundant) equal to or less than 0.01, which the conventional scheme (constant weighting) is difficult to use practically and the variable weighting scheme by Bird [22] is comparably inaccurate in short period of running time.

2. ECWS is shown to be effective and accurate in DSMC simulation with gas-phase reactions with trace species and surface reactions with very small reaction probability, which are both otherwise impossible to model using conventional scheme.
3. ECWS using TCE model and that proposed by Boyd and Stark [19] in DSMC simulation produce similar results in simulating the chemical reaction rate for silane decomposition in gas phase.
4. In the temperature range of 800–1500 K, satisfied results of rate coefficients by DSMC simulation are obtained if IDOF = 11 is used for silane decomposition.

From the results of the current study, it can be concluded that the ECWS is highly potential in simulating reactive flows using DSMC involving gas-phase if there is any critical trace species present and surface reactions if low surface reaction probability involved. Note that the ECWS can be applied to treat plasma-enhanced CVD flows involving critical trace species in a similar way. In addition, simulating the chemical deposition onto a single wafer by a downward impinging jet (e.g. a typical LPCVD chamber), using DSMC incorporating ECWS, is currently in progress and will be reported in the near future.

REFERENCES

1. Hitchman E, Jensen K. *Chemical Vapour Deposition: An Overview in Chemical Vapour Deposition: Principles and Applications*. Hitchman M, Jensen K (eds). Academic Press: New York, 1993.
2. Coronell DG. Simulation and analysis of rarefied gas flows in chemical vapour deposition processes. *Ph.D. Thesis*, MIT, 1993.
3. Kleijn CR. A mathematical model of the hydrodynamics and gas-phase reactions in silicon LPCVD in a single-wafer reactor. *Journal of the Electrochemical Society* 1991; **138**(7):2190–2200.
4. Coltrin ME, Kee RJ. A mathematical model of the gas-phase and surface chemistry in GaAs MOCVD. *Material Research Society Symposium Proceedings* 1989; **145**:119.
5. Coltrin ME, Kee RJ, Evans GH. A mathematical model of the fluid mechanics and gas-phase chemistry in a rotating-disk chemical vapour deposition reactor. *Journal of the Electrochemical Society* 1989; **136**(3):819–829.
6. Moffat HK, Jensen KF. Three-dimensional flow effects in silicon CVD in horizontal reactors. *Journal of the Electrochemical Society* 1988; **135**(2):459–471.
7. Wang YB, Chaussavoine C, Teyssandier F. 2D modelling of a non-confined circular impinging jet reactor; Si chemical vapour deposition. *Journal of Crystal Growth* 1993; **126**:373–395.
8. Coronell DG, Jensen KF. Simulation of rarefied gas transport and profile evolution in nonplanar substrate chemical vapour deposition. *Journal of the Electrochemical Society* 1994; **141**(9):2545–2551.
9. Nanbu K, Igarashi S, Watanabe Y. Molecular simulation of film growth rate in the low-pressure CVD method. *JSME International Journal Series B-Fluids & Thermal Engineering* 1990; **56**(524):892–897.
10. Nanbu K, Mitamura S, Igarashi S. Growth rate of silicon films on a wedge-shaped substrate in the LP-CVD reactor. *JSME International Journal Series B-Fluids & Thermal Engineering* 1991; **57**(542):3526–3530.
11. Nanbu K, Sugawara T, Igarashi S. Monte Carlo simulation of the growth rate of films in a CVD diffusion reactor. *JSME International Journal Series B-Fluids & Thermal Engineering* 1991; **57**(543):3760–3764.
12. Ikegawa M, Kobayashi J. Semiconductor deposition profile simulation using direct simulation Monte Carlo method. *JSME International Journal Series B-Fluids & Thermal Engineering* 1993; **59**(567):3365–3371.
13. Masato I, Junichi K. Deposition profile simulation using the direct simulation. *Journal of the Electrochemical Society* 1989; **136**(10):2982–2986.
14. Nance RP. Monte Carlo simulation of three-dimensional hypersonic flows on parallel architectures. *Master Thesis*, North Carolina State University, 1995.
15. Kannenberg KC. Computational method for the direct simulation Monte Carlo technique with application to plume impingement. *Ph.D. Thesis*, Cornell University, Ithaca, NY 1998.
16. Plimpton S, Bartel T. Parallel particle simulation of low-density fluid flows. *U.S. Department of Energy Report No.* DE94-007858, 1993.
17. Wu JS, Tseng KC. Analysis of micro-scale gas flows with pressure boundaries using direct simulation Monte Carlo method. *Computers & Fluids* 2001; **30**:711–735.
18. Bird GA. *Molecular Gas Dynamics and the Direct Simulation of Gas Flows*. Oxford University Press: New York, UK, 1994.
19. Boyd ID, Stark JPW. Direct simulation of chemical reactions. *Journal of Thermophysics* 1990; **4**(3):391–393.

20. Boyd ID. Conservative species weighting scheme for the direct simulation Monte Carlo method. *Journal of Thermophysics and Heat Transfer* 1996; **10**(4):579–585.
21. Sakiyama Y, Takagi S, Matsumoto Y. Full simulation of silicon chemical vapour deposition process. In *22nd International Symposium on Rarefied Gas Dynamics*, Bartel TJ, Gallis MA (ed.). 2000; 206–213.
22. Bird GA. *Molecular Gas Dynamics*. Oxford University Press: Oxford, England, UK, 1976.
23. Bird GA. Monte Carlo simulation in an engineering context. In *Progress in Astronautics and Aeronautics: Rarefied Gas Dynamics*, vol. 74, Pt. 1, Sam S. Fisher (ed.). AIAA: New York, 1981; 239–255.
24. Hsu CC. Molecular simulation of monosilane gas-phase decomposition and diffusion by DSMC. *Master Thesis*, Department of Chemical Engineering, National Taiwan University of Science and Technology, 1997.

